



POLYTECHNIQUE  
MONTREAL

LE GÉNIE  
EN PREMIÈRE CLASSE

# Validation of an Isotope Evolution Model for APOLLO3 Calculations in SFR Core

Aaron GREGANTI

aaron.greganti@polymtl.ca

*ÉCOLE POLYTECHNIQUE DE MONTRÉAL*  
*in collaboration with*  
*CEA / DER / SPRC*

*Mars 10<sup>th</sup>, 2017*



In this thesis work, depletion calculations have been performed in a Coeur à Faible Vidange (CFV), proper of ASTRID fast reactor. The following models have been used:

- ▶  $\sigma_0$  **Micro Depletion Model**
- ▶ **Macro Depletion Model**
- ▶  $\sigma(t)$  **Micro Depletion Model**

## Research Question

“Is the ECCO/ERANOS  $\sigma_0$  model accurate enough to describe the isotope evolution in CFV core configuration with the aid of APOLLO3 code?”

## Introduction

Background

Transport Calculations

Depletion Calculations

Depletion Models

Evolution of a CFV Cell Geometry

Evolution of a Fissile-Fertile Cluster Geometry

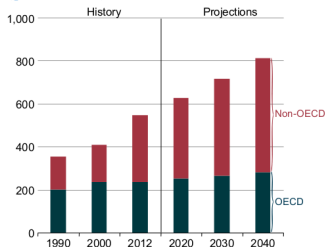
Evolution of a 2D Core Plane Geometry

Conclusion

Appendices

# Growing of Energy Demand

Figure 1-1. World energy consumption, 1990–2040 (quadrillion Btu)

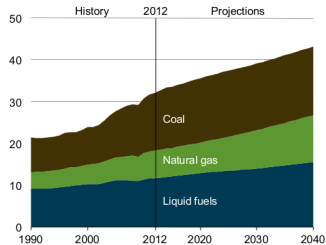


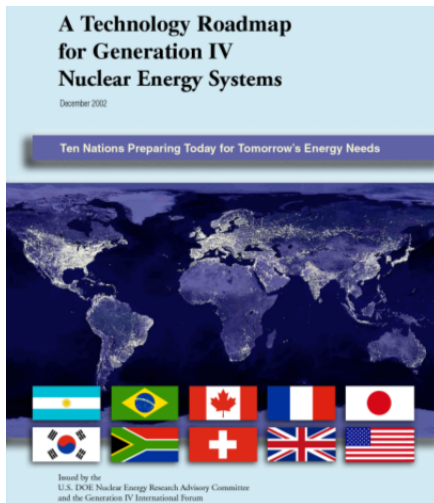
The graph is taken from the *International Energy Outlook 2016*, published by the U.S. Energy Information Administration (EIA). It shows the behaviour of energy consumption throughout the years, with reasonable projections for the future.

$$\begin{aligned}
 1 \text{ quadrillion BTU} &= 33.434 \text{ GWy} \\
 &= 1.055 \cdot 10^{18} \text{ J}
 \end{aligned}$$

If more energy is demanded, more energy is produced. But, for the time being, each way to produce electricity consumes natural resources and somehow alters natural ecosystems. This anthropic effect must be reduced to minimum in order to assure a sustainable development. The example of the carbon dioxide emission (CO<sub>2</sub>) is only one of the environmental issues that have come up to the collective consciousness in the recent years.




























Figure ES-8. World energy-related carbon dioxide emissions by fuel type, 1990–2040 (billion metric tons)





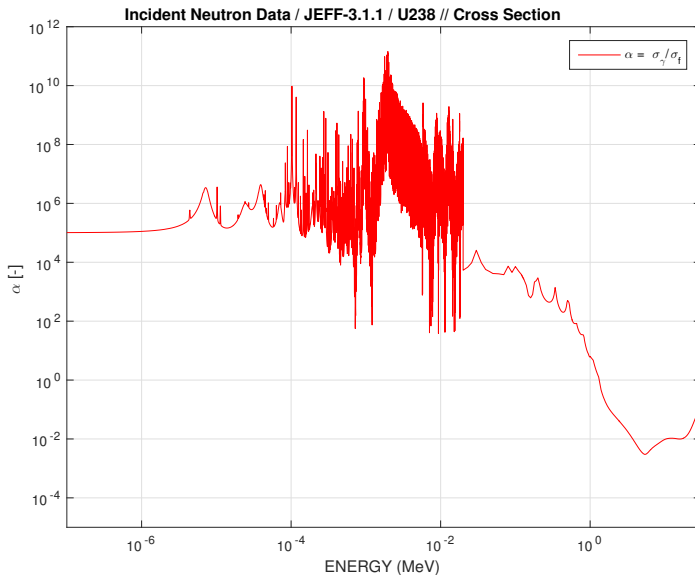
- ▶ **Sustainability:** Generation IV energy systems must decrease CO<sub>2</sub> production and reduce polluting emissions. They must exploit better the natural resources in order to minimize nuclear waste production.
- ▶ **Economics:** Generation IV energy systems must be competitive with respect to the ones exploiting other energy sources.
- ▶ **Safety and Reliability:** Generation IV energy systems must be more safe and reliable. Severe accidents less probable and no offsite energy response are key features of these systems.
- ▶ **Proliferation Resistance and Physical Protection:** Generation IV energy systems must be an unattractive way to produce weapon usable materials, and they must provide enhanced physical protection against act of terrorism.

# Generation IV International Forum Nuclear Reactor Systems

GIF member	System arrangement				MOU <sup>a</sup>	
	GFR	SCWR	SFR	VHTR	LFR	MSR
Canada						
China						
European Union						
France						
Japan						
Korea						
Russia						
Switzerland						
United States						
No. of Projects	1	2	5	3	—	—
Demonstration phase begins	>2030	2025	2022	2025	2022	>2030

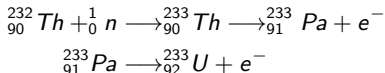
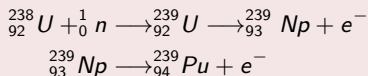
<sup>a</sup> Memorandum of Understanding, a provisional arrangement for collaboration.





Fast spectrum reduces  $\alpha = \sigma_{\gamma}/\sigma_f$  ratio. This fact, along with the increase of the average number of secondary neutron produced  $\nu$ , allows to have a spare neutron to **fertilize a fissionable nuclei** or to **burn a minor actinide**.

The following are the transmutation reactions of the most common fissionable nuclei:

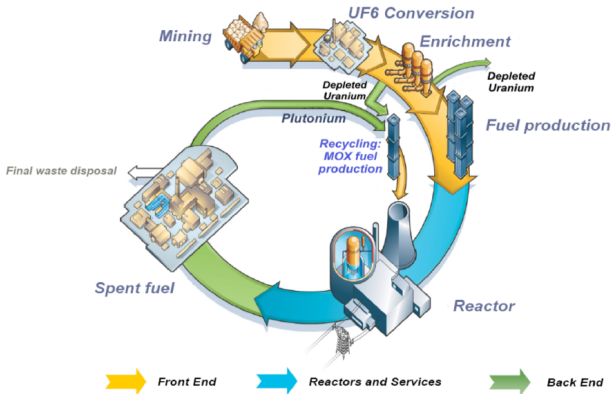


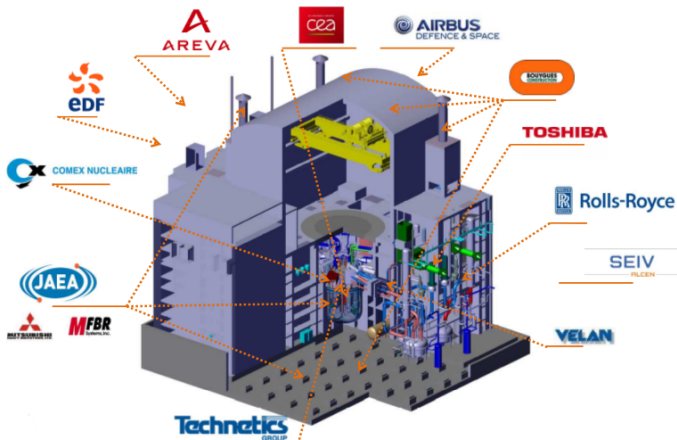
## Advanced Sodium Technological Reactor for Industrial Demonstration

In June 2006, French government passed a law focused on the disposition of long life high activity waste. A prototype, **capable of transmutation and separation of long life isotopes**, was scheduled for the end of 2020. ASTRID project began and CEA was given the responsibility for the operational management, core design and R& D work.

# ASTRID

## Fuel Closed Cycle



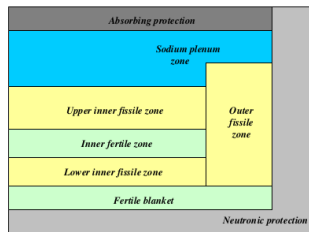
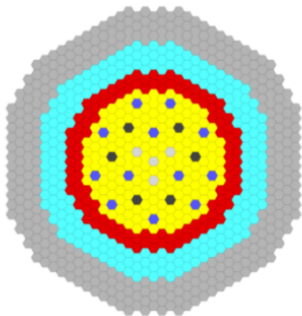


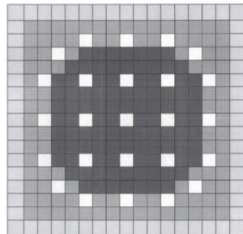
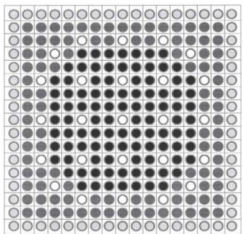
## Coeur à Faible Vidange

The core conception of the ASTRID project is one of enhanced safety. It guarantees **limited power excursion** if fuel temperature increases (Doppler effect) and **it does not assure a reactivity gain if sodium boils or core is completely drained**.

This conception satisfies the following objectives:

- ▶ favourable transient in case of unprotected loss of flow and heat sink
- ▶ no sodium boiling in case of unprotected loss of station supply power (ULOSSP)
- ▶ favourable behaviour in case of control rod withdrawal (CRW)







- ▶ reference Monte Carlo code: **TRIPOLI4**
- ▶ **APOLLO2/CRONOS2**: chain of nuclear codes for thermal and epithermal reactors
- ▶ **ECCO/ERANOS**: chain of nuclear codes for fast reactors

APOLLO3 is a new code whose key objective is to merge together the lattice and core steps in one single code, in order to accomplish one step calculations in the future. In order to do so, computer architectures must be exploited at their best. Main objectives are the following:

- ▶ **Flexibility:** from high precision calculations to industrial design
- ▶ **Easy coupling** with Monte Carlo and Thermohydraulical/  
Thermomechanical codes, including coupling with the SALOME platform
- ▶ **Extended application domain:** performing criticality and shielding calculations for all kinds of reactors (a multi spectrum code for FNR, PWR and experimental reactors)
- ▶ **Uncertainties assessments** using perturbation methods

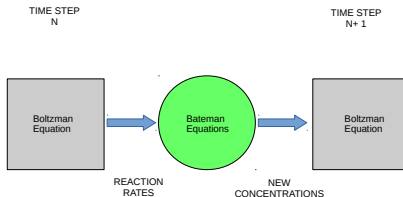
CFV simulation presents problems in the correct representation of the following elements:

- ▶ **radial blanket** loaded with minor actinides
- ▶ **neutron shielding** and **reflector**
- ▶ **sodium plenum** and **fertile plate**
- ▶ flux distribution in a core with outer core height greater than inner one (**Diabolo effect**)

In order to supply a reliable code to users and designers, a rigorous method, called **VVUQ**, has been used:

- ▶ **Verification:** internal coherence and numerical results of the solvers are verified through non regression test
- ▶ **Validation:** in order to evaluate the accuracy of neutronic models and calculation schemes, comparisons with the reference Monte Carlo code TRIPOLI4 are performed
- ▶ **Uncertainty Quantification:** the global package, including APOLLO3, the codes which treat the evaluated nuclear data and the nuclear data themselves, is tested comparing it with measurements from dedicated experimental programs. Experimental uncertainties are transposed to neutronic designed parameters

In order to perform depletion calculations, **APOLLO3** is coupled with **MENDEL** depletion solver. *In steady state reactor physics, transport and depletion equations are decoupled.* They are solved independently supposing concentrations to vary slowly. This allows to use the solution of the former for the latter and vice versa.



The variation of the concentration of an isotope is equal to the difference between the rates of its production and of its transmutation due to absorption or spontaneous decay. The **source term** is:

$$S_k(t) = \sum_{j=1}^J \left[ \sum_{yg=1}^{YG} Y_{k,j}^{yg} < \sigma_{f,j} \Phi >_{yg} (t) \right] N_j(t) + \sum_{j=1}^K \lambda_{j \rightarrow k}(t) N_j(t)$$

and the **transmutation term** is equal to

$$\Lambda_k(t) N_k(t) = (\lambda_k + < \sigma_{a,k} \Phi > (t)) N_k(t)$$

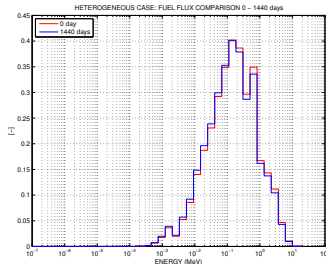
where the cross sections and the flux are integrated all over the proper energy domain. YG is the number of fission yield groups used. The first order system of K equation is

$$\frac{dN_k}{dt} + \Lambda_k(t) N_k(t) = S_k(t)$$

for  $k=1, \dots, K$ .

The **CEA-V5** depletion chain contains **126 fission products**, **26 actinides** and **5 additional isotopes**. Fission yields are defined both for thermal fission ( $< 2.5\text{KeV}$ ) and fast fission ( $> 2.5\text{KeV}$ ). While lattice calculations take into account the two groups, *core calculations are performed taking into account only the fast one*. This approximation is reasonable at all time steps. In her paper, *Sylvia Domanico* has validated the standard CEAV5 depletion chain, both for light water reactors (**PWRs**) and sodium fast reactors (**SFRs**).

- In **lattice calculations**, microscopic cross sections can vary owe to **self shielding**.
- In **core calculations**, microscopic cross sections can vary because, in the multigroup approach, they are **condensed into a coarser energy mesh** using the proper flux, which can vary at each time step.



At each time step a new flux is evaluated. The flux, for instance, after 1440 days of cell exploitation, slightly shifts towards lower energy.



The change of cross sections can be taken into account or not in core evolution, according to the model. Now, three depletion models are introduced:

- ▶ **MACRO DEPLETION MODEL:** concentrations and cross sections are stocked for each time step. Bateman equations are solved at lattice level only and stocked information on the concentrations are used.
- ▶ **MICRO SIGMA ZERO DEPLETION MODEL:** only time zero concentrations and cross sections are stocked. Bateman equations are solved also at core level.
- ▶ **MICRO SIGMA EVOLVING DEPLETION MODEL:** concentrations and cross sections are stocked for each time step. Bateman equations are solved at core level and cross sections updated at each time step.

Assuming  $\vec{L}$  to be a state vector for the fuel cell, the three depletion models can be resumed as it follows:

MACRO	$\tilde{\Sigma}(\vec{L}, t) =$	$\bar{\Sigma}(\vec{L}, t)$
MICRO SIGMA ZERO	$\tilde{\Sigma}(\vec{L}, t) =$	$\bar{\Sigma}(\vec{L}, 0) + \sum_k \tilde{N}_k(t) \bar{\sigma}_k(\vec{L}, 0)$
MICRO SIGMA EVOLVING	$\tilde{\Sigma}(\vec{L}, t) =$	$\bar{\Sigma}(\vec{L}, t) + \sum_k \tilde{N}_k(t) \bar{\sigma}_k(\vec{L}, t)$

where  $-$  means that **lattice quantities** are considered while  $\sim$  is related to **core quantities**.

## Introduction

### Evolution of a CFV Cell Geometry

Lattice Depletion

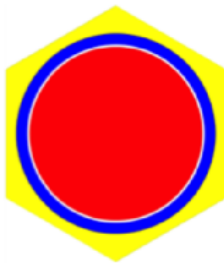
Core Depletion

### Evolution of a Fissile-Fertile Cluster Geometry

### Evolution of a 2D Core Plane Geometry

## Conclusion

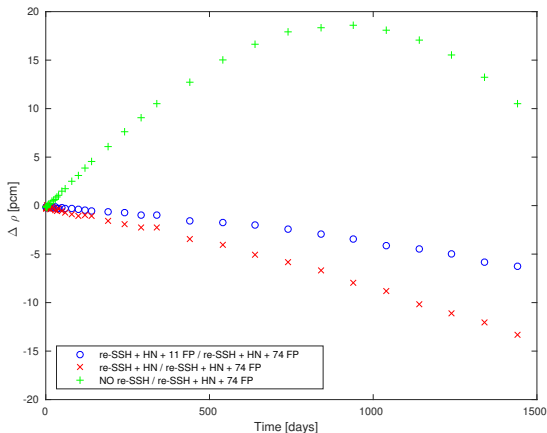
## Appendices



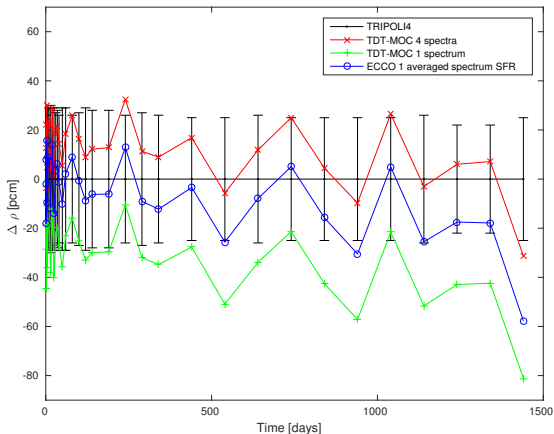
Lattice calculations are performed using TDT-MOC solver, whereas core calculations use the MINARET Sn one. The former will constitute the references our models will be compared with. 1 energy spectrum for fission neutrons has been used in our lattice calculations. For the time being, in fact, it is not possible to perform multi-spectrum core calculations.

# Lattice Depletion

## Preliminary Studies: Self-Shielding Iteration



TRIPOLI4 and APOLLO3 are related to the same depletion solver: **MENDEL**. Consequently, they can be affected from the same bias. ERANOS depletion solver has been introduced in the validation process to offer a further guarantee.

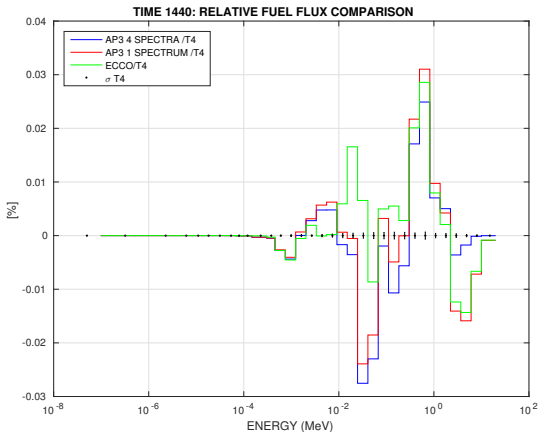


The number and the type of fission spectra have a dominant role in the neutron balance.

TDT-MOC calculations with 4 spectra are coherent with TRIPOLI4 results because fission reactions are correctly estimated for U238 (threshold reaction).

Pu239 secondary neutron spectrum is harder if 4 spectra are considered instead of 1.





The Iterated Fission Probability method (**IFP**) implemented in TRIPOLI4 has been used by Sylvia Domanico to enlist a hierarchy of the fission products (**FPs**) concerning their contribution to the total amount of anti-reactivity.

In the APOLLO3 calculations presented, a reconstruction of the global balance in the multiplicative geometry has been done for reference calculations. The FP hierarchy found is coherent with the one by Domanico.

$$k_{inf} = \frac{PROD_{tot}}{ABS_{tot} - NEXC_{tot}}$$

with

$$NEXC_{tot} \ll ABS_{tot}$$

$$PROD_{tot} = \sum_{r=1}^R \sum_{i=1}^{N_f^r} \sum_{g=1}^G \tau_{prod}^{r,i,g}$$

$$ABS_{tot} = \sum_{r=1}^R \sum_{i=1}^{N_f^r} \sum_{g=1}^G \tau_{abs}^{r,i,g}$$

$$NEXC_{tot} = \sum_{r=1}^R \sum_{i=1}^{N_f^r} \sum_{g=1}^G \tau_{nexc}^{r,i,g}$$

$$\begin{aligned} \Delta\rho &= \frac{1}{k_{inf}^1} - \frac{1}{k_{inf}^2} \approx \frac{ABS_{tot}^1}{PROD_{tot}^1} - \frac{ABS_{tot}^2}{PROD_{tot}^2} = \\ &= \sum_{r=1}^R \sum_{i=1}^{N_f^r} \sum_{g=1}^G \left( \frac{(\tau_{abs}^{r,i,g})^1}{PROD_{tot}^1} - \frac{(\tau_{abs}^{r,i,g})^2}{PROD_{tot}^2} \right) \end{aligned}$$

$$RD^{i,r} = \sum_{g=1}^G \left( \frac{(\tau_{abs}^{r,i,g})^1}{PROD_{tot}^1} - \frac{(\tau_{abs}^{r,i,g})^2}{PROD_{tot}^2} \right)$$

$$\Delta\rho = \sum_{r=1}^R \sum_{i=1}^{N^r} RD^{i,r}$$

The importance of isotope  $i$  belonging to region  $r$  is:

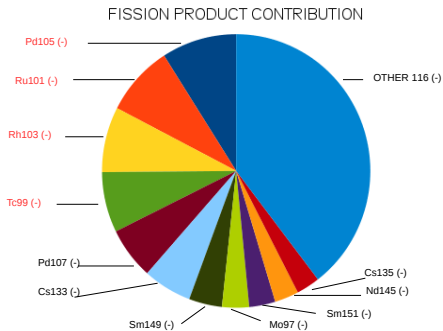
$$I = \frac{RD^{r,i}}{\Delta\rho^*}$$

where  $\rho^*$  can be the overall reactivity or the one due to a group of few isotopes, e.g. the reactivity difference only related to fission products ( $\Delta\rho_{FP}$ ).

From lattice MOC calculations it is possible to show the following:

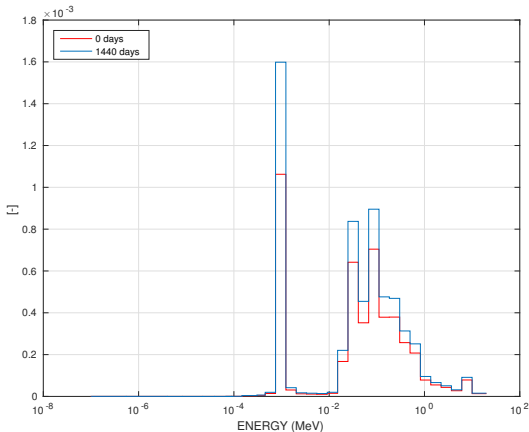
	$\Delta\rho[pcm]$	rel
ACTINIDES	-4669	-41.26%
FP	-6189	-54.72%
STRUCTURES	-455	-4.02%
ABSORPTION LOSS	-11313	
NEXCESS GAIN	+17	
OVERALL LOSS	-11296	

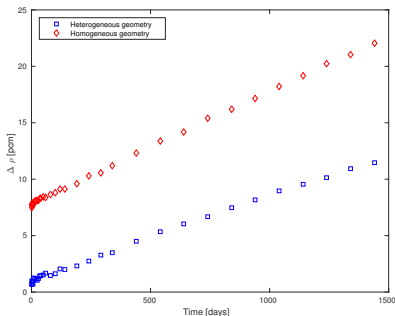
The reactivity loss in the STRUCTURES is due principally to an increasing of Fe56 reaction rate between 1.2-2 keV caused by the flux shifting towards lower energy.



# Lattice Depletion

## Reactivity Analysis - Absorption Fe56 at 1440 days





An evolution with the cross section condensed at 1968g at time 0 is performed. The derive of the multiplication factor, *compared to a MOC calculation where self shielding is not repeated* at each time step, is equal to **15pcm in heterogeneous geometry** and **10pcm in homogeneous one**.



	Lattice	Core
Solver	TDT	MINARET
Method	MOC	Sn
Energy Group	1968	33
Fission Yields	2	1
Fission Spectra	1/4	1

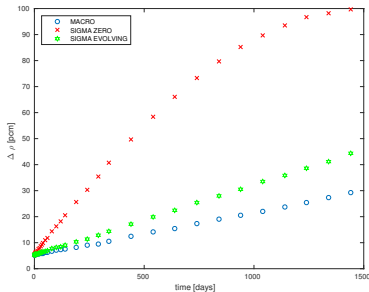
The following table presents the multiplication factors for lattice MOC calculations at 1968g and Sn calculations at 33g and their difference with respect to the reference one at time zero:

	HET		HOM	
	$k_{eff}$	$\Delta\rho[pcm]$	$k_{eff}$	$\Delta\rho[pcm]$
REFERENCE: MOC 1968g	1.54580	/	/	/
CORE TIME 0: Sn 33g	1.54593	5	1.54581	0.5

**Heterogeneous case:** the 4 *regions* of the cell are preserved in core calculations.

**Homogeneous case:** 1 *region* cell is considered for core calculations.

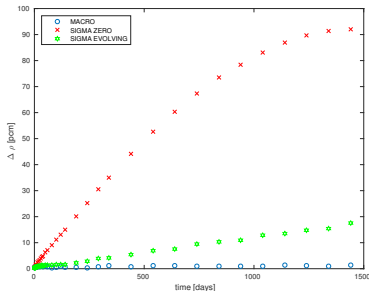
# CFV Cell Geometry: No Leakage Heterogeneous Case



Results at 1440 days

	$k_{eff}$	$\Delta\rho[pcm]$
reference	1.31600	/
MACRO	1.31651	29
SIGMA ZERO	1.31773	100
SIGMA EVOLVING	1.31677	44

# CFV Cell Geometry: No Leakage Homogeneous Case



Results at 1440 days

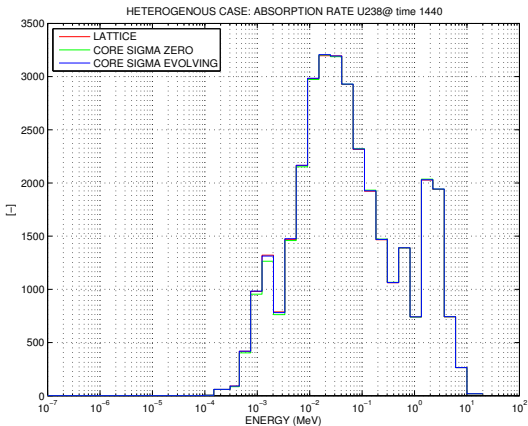
	$k_{eff}$	$\Delta\rho[pcm]$
reference	1.31600	/
MACRO	1.31603	1
SIGMA ZERO	1.31760	92
SIGMA EVOLVING	1.31631	18

		SIGMA ZERO [pcm] 33g	SIGMA EVOLVING [pcm] 33g
HOM	U238	+123	-2
	Pu239	+11	+0.5
	Fe56	+7	-0.2
HET	U238	+123	-5
	Pu239	+12	-3
	Fe56	+7	-10

Evolving the microscopic cross sections is a possible way to reduce the reactivity differences.

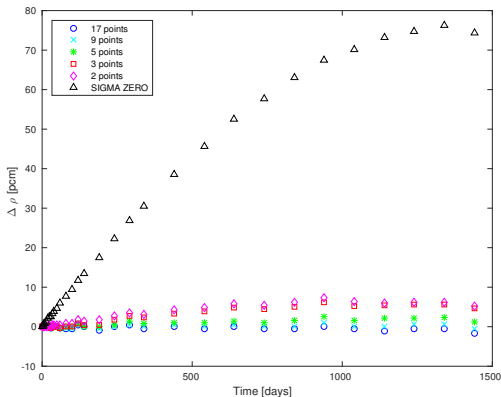
# CFV Cell Geometry: No Leakage

Time: 1440 days



# CFV Cell Geometry: No Leakage

## Burn-up Parametrization of the Cross Section Libraries

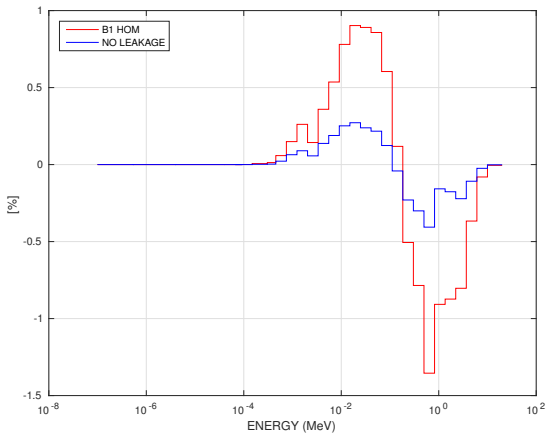


*Using a MICRO SIGMA EVOLVING model with 2 point cross section library gives a final difference equal to +23 pcm (only +5 pcm with respect to the reference case with 34 points).*

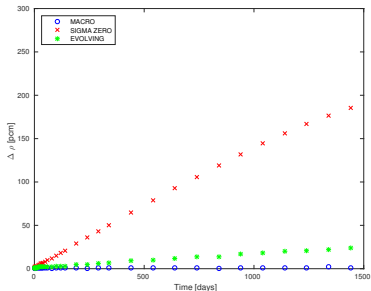
In order to subsequently perform full core calculations, leakage models are applied to lattice calculations. They simulate a finite reactor geometry, even if an infinite lattice is considered. Applying an **homogeneous B1 leakage model** to a single cell, a softening of the flux is observed even in this case. *The flux softens more in this case with respect to the one without leakage model.* **MICRO SIGMA ZERO**, then, is expected to be less accurate in the representation of the time evolution of a cell.



# CFV Cell Geometry: Leakage Flux Shifting



# CFV Cell Geometry: Leakage Homogeneous Case



## Results at 1440 days

	$k_{eff}$	$\Delta\rho[pcm]$
reference	0.99997	/
MACRO	0.99998	1
SIGMA ZERO	1.00183	185
SIGMA EVOLVING	1.00021	24

The flux shifting modifies the cross sections. Evolving them means decreasing the reactivity difference in time evolution.

	SIGMA ZERO [pcm] 33g	SIGMA EVOLVING [pcm] 33g
U238	+165	+3
Pu239	+61	0
Pu240	+10	+1
Fe56	+6	0

Introduction

Evolution of a CFV Cell Geometry

Evolution of a Fissile-Fertile Cluster Geometry

Lattice Depletion

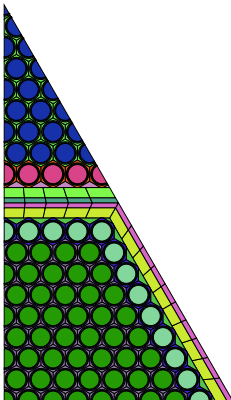
Core Depletion

Evolution of a 2D Core Plane Geometry

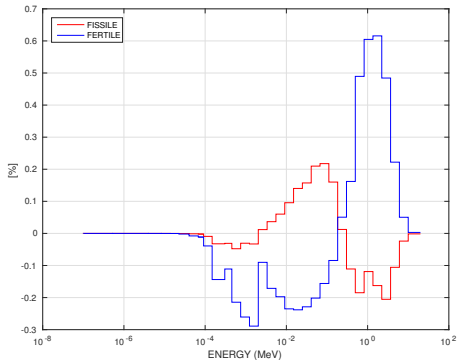
Conclusion

Appendices

A cluster fissile-fertile is now considered



As in the cell case the flux spectrum is softened during the evolution in the fissile zone.

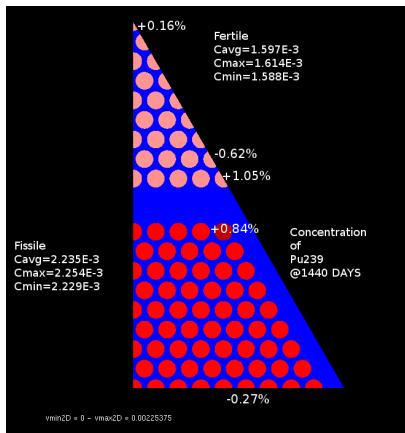


Neutron energy, on the contrary, increases during flux evolution in fertile zone.

Before introducing the results of the considered depletion models, it is interesting to answer the following question: **during the evolution, do geometrical asymmetries arise, which can require particular homogenization geometry for core calculations? Is an overall homogenization of the fissile and fertile zone accurate enough?**

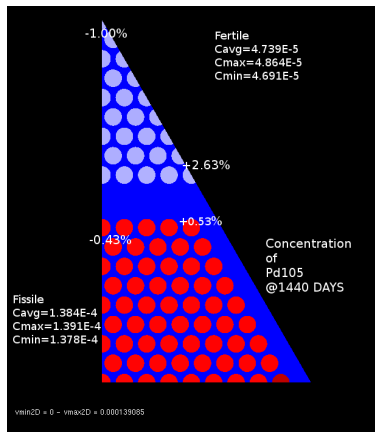
In lattice calculations, *evolving each cell independently or evolving separately only the external ring do not affect the multiplication factor*. At the end of the evolution cycle, no asymmetries arise, as it is possible to see for the concentration map of Pu239 and Pd105.

# Lattice Depletion Reference Evolution Geometry

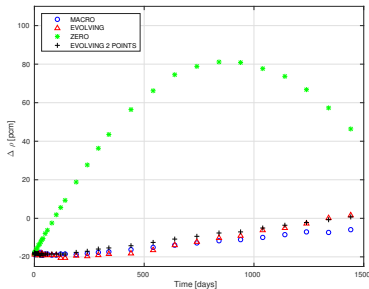




# Lattice Depletion Reference Evolution Geometry



# Fissile-Fertile Cluster Geometry Homogeneous Case



## Results at 1440 days

	$k_{eff}$	$\Delta \rho [pcm]$
reference	1.16629	/
MACRO	1.16621	-6
SIGMA ZERO	1.16692	+46
SIGMA EVOLVING	1.16631	+1
SIGMA EVOLVING 2 POINTS	1.16630	+0

Evolving the cross sections leads to a better representation of the reaction rates of the isotopes enlisted below.

		SIGMA ZERO [pcm] 33g	SIGMA EVOLVING [pcm] 33g
Fertile	U238	+94	+2
	Pu239	-3	+22
	Pu240	-5	+3
	Fe56	+5	+1
Fissile	U238	+131	-8
	Pu239	-6	-19
	Pu240	-32	-4
	Fe56	+12	-1

On the contrary, Pu239 is worsely represented, but a compensation occurs between the fissile and fertile regions.

## Introduction

## Evolution of a CFV Cell Geometry

## Evolution of a Fissile-Fertile Cluster Geometry

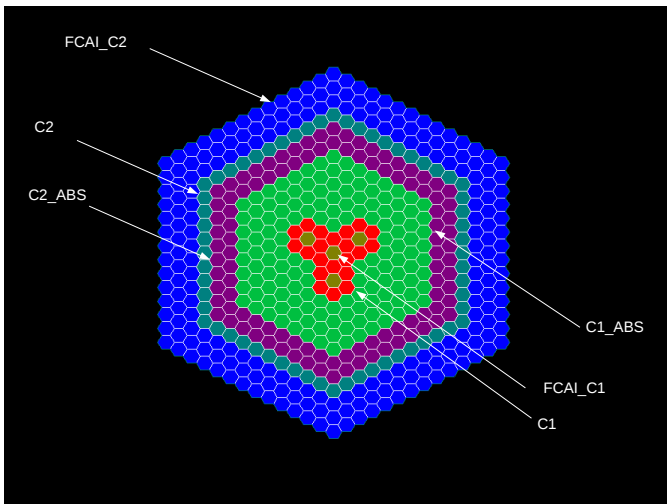
## Evolution of a 2D Core Plane Geometry

How is the reactivity difference associated to the MICRO SIGMA ZERO model propagated throughout the core?

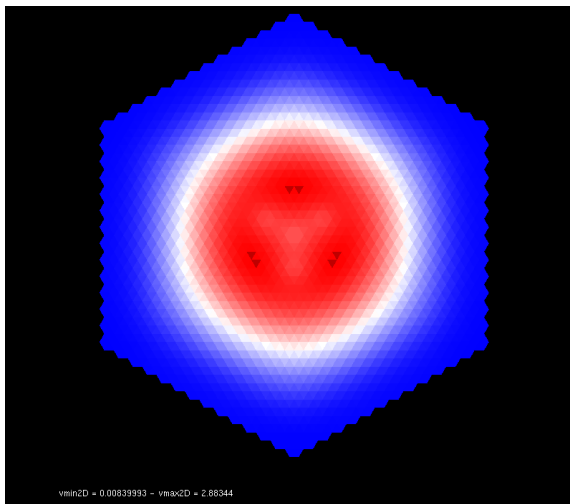
## Conclusion

## Appendices

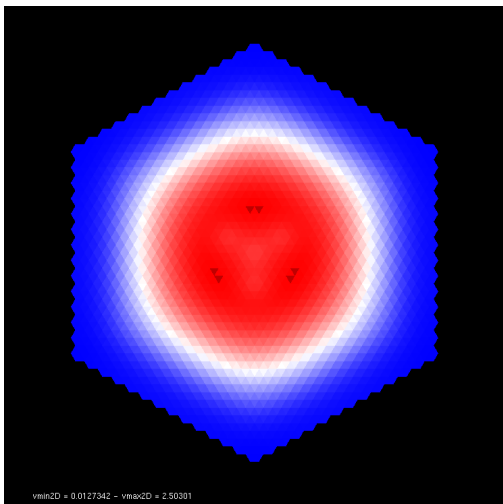
# 2D Core Plane Geometry



# 2D Core Plane Geometry Initial Time



The multiplication factor at time zero is equal to **1.40728**. The outer C1 fissile region presents the flux peak, whereas the lowest value of the flux is, obviously, in the external ring of the lattice. *The peak is **340** higher than the lowest value.* A depression of the flux is present in the inner fertile region. The flux is *normalized to a total power of **10 MW/cm** and after 1440 days a reactivity loss equal to 6567 pcm is accounted.* *The ratio between the flux peak and its lowest value is reduced to **197**.*

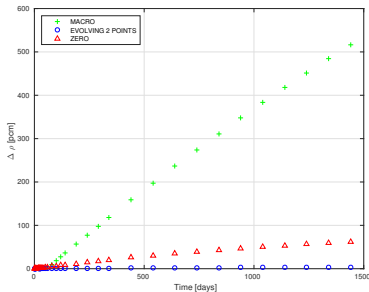




## 2D Core Plane Geometry

Comparisons of isotope concentrations and flux at 1440 days

	Peak/Lowest Value Ratio			Peak/Inner Fertile Averaged Value		
	EVOLVING	ZERO	MACRO	EVOLVING	ZERO	MACRO
U238	1.405	1.405	1.406	1.071	1.071	1.071
U235	2.191	2.192	2.224	1.734	1.739	1.734
Pu239	225	225	2177	2.645	2.651	2.679
Pd105	12665	12699	16608	5.238	5.246	5.290
Tc99	2201	2207	13166	4.032	4.043	4.351
Ru101	4540	4553	3450	4.449	4.462	4.589
Rh103	8699	8722	157136	4.766	4.778	5.025
Flux	197	197	199	1.088	1.087	1.090



## Results at 1440 days

	$k_{eff}$	$\Delta\rho[pcm]$
SIGMA EVOLVING	1.28822	/
MACRO	1.29684	+516
SIGMA ZERO	1.28924	+61
SIGMA EVOLVING 2 POINTS	1.28828	+4

Introduction

Evolution of a CFV Cell Geometry

Evolution of a Fissile-Fertile Cluster Geometry

Evolution of a 2D Core Plane Geometry

Conclusion

Appendices

## Research Question

"Is the ECCO/ERANOS  $\sigma_0$  model accurate enough to describe the isotope evolution in CFV core configuration with the aid of APOLLO3 code?"

Previous results have shown that lattice calculations or core calculations at 1968g are not sensitive to successive self shielding of microscopic cross sections. Difference are less than 20 pcm.

Considering, on the contrary, a condensation into a coarser energy mesh (33g), reactivity difference applying the  $\sigma_0$  model are of the order of 100 pcm, *but it can double if a leakage model is used.*

*In conclusion, the MICRO SIGMA ZERO model has not been validated. To this model, a **MICRO SIGMA EVOLVING one with two burn-up tabulation points** in the microscopic cross section libraries is preferred. An higher accuracy of the results is reached *only by doubling* the calculation time at lattice step and the memory storage. Of course, these conclusions are limited to the cases here considered. Future work must be done to validate the model in presence of leakage and for 3D geometries. A study of the whole CFV configuration is also suggested.*

Thank you  
**Q & A**

Introduction

Evolution of a CFV Cell Geometry

Evolution of a Fissile-Fertile Cluster Geometry

Evolution of a 2D Core Plane Geometry

Conclusion

## Appendices

Appendix: Transport Calculations

Appendix: Flux Normalization

Appendix: Depletion Solver

Appendix: Evolution of a 2D Core Plane Geometry

The Boltzmann transport equation is the following:

$$\vec{\Omega} \cdot \vec{\nabla} \phi(\vec{r}, E, \vec{\Omega}, t_N) + \Sigma(\vec{r}, E, t_N) \phi(\vec{r}, E, \vec{\Omega}, t_N) = Q(\vec{r}, E, \vec{\Omega}, t_N)$$

where the source density is:

$$Q(\vec{r}, \vec{\Omega}, v_n, t_N) = Q_{scatt}(\vec{r}, E, \vec{\Omega}, t_N) + \frac{1}{4\pi k} Q_{fiss}(\vec{r}, E, t_N)$$

In the assumption of isotropic materials, and neglecting  $t_N$  in the notation from now on:

$$Q_{scatt}(\vec{r}, E, \vec{\Omega}) = \frac{1}{2\pi} \int_{4\pi} d^2\Omega' \int_0^{+\infty} dE' \Sigma_s(\vec{r}, E \leftarrow E', \vec{\Omega} \cdot \vec{\Omega}') \phi(\vec{r}, E', \vec{\Omega}')$$

where a Legendre polynomial expansion can be performed on scattering cross section.



In order to reduce the number of variables, a multigroup approach is used. This approach results in the utilization of energy averaged quantities.

The G transport equations are:

$$\vec{\Omega} \cdot \vec{\nabla} \Phi_g(\vec{r}, \vec{\Omega}) + \Sigma_g(\vec{r}) \Phi_g(\vec{r}, \vec{\Omega}) = Q_g(\vec{r}, \vec{\Omega})$$

for  $1 \leq g \leq G$ .

The quantities of interest are

$$\phi^g(\vec{r}) = \int_{4\pi} d^2\Omega \phi^g(\vec{r}, \vec{\Omega}) = \int_{4\pi} d^2\Omega \int_{E_{g+1}}^{E_g} dE \phi(\vec{r}, E, \vec{\Omega})$$

$$\Sigma^g(\vec{r}) = \frac{1}{\phi^g(\vec{r})} \int_{E_{g+1}}^{E_g} dE \Sigma(\vec{r}, E) \phi(\vec{r}, E)$$

$$\Sigma_s^{g' \rightarrow g}(\vec{r}, \vec{\Omega}' \cdot \vec{\Omega}) = \frac{1}{\phi^{g'}(\vec{r}, \vec{\Omega}')} \int_{E_{g+1}}^{E_g} dE \int_{E_{g'+1}}^{E_{g'}} dE' \Sigma_s(\vec{r}, E' \rightarrow E, \vec{\Omega}' \cdot \vec{\Omega}) \phi(\vec{r}, \vec{\Omega}', E')$$

In reference **TRIPOLI4** calculations, the fission source density is accurately represented by the **multigroup fission matrix**. The fission term becomes:

$$Q_{fiss}^g(\vec{r}) = \sum_{j=1}^J \sum_{g'=1}^{G'} N_j(\vec{r}) \sigma_{f,j}^{g' \rightarrow g} \phi^{g'}(\vec{r})$$

where  $J$  is the number of fissile isotopes.

In **APOLLO3** calculations, **fission spectra** are used instead. *If one fission spectrum is used, the dependency of the secondary neutron fission spectrum on the incident neutron energy is neglected.* The fission source term is written as follows:

$$Q_{fiss}^g(\vec{r}) = \sum_{j=1}^J \chi_j^g \sum_{g'=1}^{G'} N_j(\vec{r}) \nu_j^{g'}(\vec{r}) \sigma_{f,j}^{g'}(\vec{r}) \phi^{g'}(\vec{r})$$

The secondary neutron fission spectrum  $\chi_j^g$  is an averaged quantity. Using a proper weighting function  $w^{g'}$ :

$$\chi_j^g = \frac{\sum_{g'=1}^{G'} \sigma_{f,j}^{g' \rightarrow g} w^{g'}}{\sum_{g'=1}^{G'} \nu_j^{g'} \sigma_{f,j}^{g'} w^{g'}}$$

In **APOLLO3 calculations**, the incident neutron energy can be considered if more than one spectrum are used. Dividing the incident neutron energy in a number  $NMG$  of macro-groups, the fission term becomes:

$$Q_{fiss}^g(\vec{r}) = \sum_{j=1}^J \sum_{mg=1}^{NMG} \chi_{j,mg}^g \sum_{g'=Inf(mg)}^{Sup(mg)} N_j(\vec{r}) \nu_j^{g'}(\vec{r}) \sigma_{f,j}^{g'}(\vec{r}) \phi^{g'}(\vec{r})$$

$Inf(mg)$  and  $Sup(mg)$  are respectively the upper and lower boundaries of the macro-group  $mg$ .

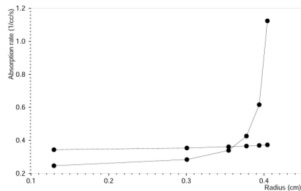
For fast neutron system,

**4 macro-group** secondary neutron fission spectra have been demonstrated to be accurate enough for the fission source representation.

	$Sup(mg)$		$Inf(mg)$
I	20 MeV	-	1.35 MeV
II	1.35 MeV	-	497 keV
III	497 keV	-	183 keV
IV	183 keV	-	$10^{-5}$ eV

In the multigroup approach, energy averaged quantities are used. Input libraries are evaluated using a weighting function  $w_g$  to average the cross sections over the energy group  $g$ .

**In a nuclear reactor, the spatial distribution of the flux is also important and its energy spectrum can vary during the evolution.**



Self-shielding models are applied in deterministic code in order to create *spatial and time dependent cross section libraries*  $\bar{\sigma}_{x,i,T}(E, \vec{r}, t_N)$ .

The **sub-group method** is applied. It consists in dividing each energy group  $g$  in  $k$  sub-groups. Riemann integrals are transformed in Lebesgue integrals and solved with a quadrature formula.

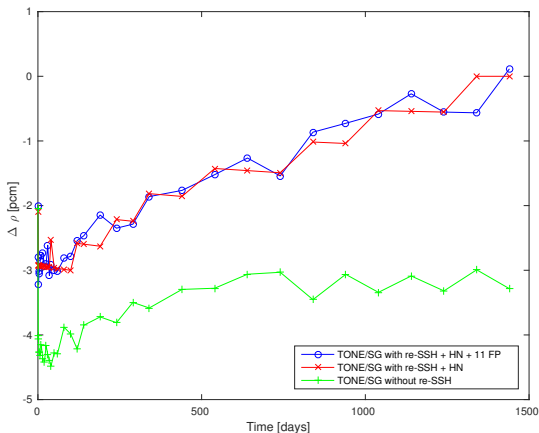
*In this work, an input library with 1968 energy groups has been used for lattice calculations.* This refined energy mesh allows to assume the **Narrow Resonances (NR)** approximation.

In the traditional **sub-group method**, the flux is evaluated using the **Collision Probability Method (CPM)**. For each sub-group  $k$  a collision probability  $p_{ij,k}^g$  is evaluated.

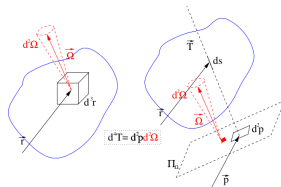
This is not true for the **Tone method**. Only 1 collision probability  $p_{ij}^g$  is evaluated. The time saved is of the order of a factor 30.

$$\phi_{ij}(u) = \frac{V_i}{V_j} \frac{P_{ij}(u)}{\Sigma_j(u)} Q_i(u) \approx \alpha_j(u) \phi_{ij}^g$$

Nevertheless, this assumption means that the treated region is “distant” or slightly sensitive to the presence of other materials. This assumption is reasonable in CFV core configuration.



In **lattice calculations**, the flux is evaluated using the **Method of Characteristics (MOC)** implemented in the TDT solver. *1968 energy groups are used.* The geometry is firstly opportunely tracked.



In each sub-domain  $k$  of length  $L_k$ , applying a Step Characteristics (SC) scheme, a **transmission** and **balance** equations are instituted:

$$\phi_{k+1}^g(\vec{r}) = \phi^g(s_{k+1}, \vec{r}) = \phi_k^g(\vec{r})e^{-\tau_{k,opt}^g} + Q_k^g(\vec{\Omega}) \frac{1 - e^{-\tau_{k,opt}^g}}{\Sigma_k^g(\vec{p})}$$

$$L_k \bar{\phi}_k(\vec{r}) = \int_{s_k}^{s_{k+1}} ds \phi(s, \vec{r}) = \phi_k(\vec{r}) \frac{1 - e^{-\tau_{k,opt}^g}}{\Sigma_k^g(\vec{p})} + Q_k^g(\vec{\Omega}) \frac{L_k}{\Sigma_k^g(\vec{p})} \left( 1 - \frac{1 - e^{-\tau_{k,opt}^g}}{\tau_{k,opt}^g} \right)$$

with  $\tau_{k,opt}^g = \int_{s_k}^{s_{k+1}} ds \Sigma_k^g(\vec{p}) = L_k \Sigma_k^g(\vec{p})$ .



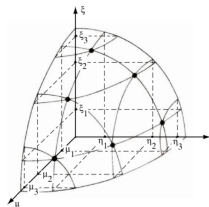
In **core calculations**, the flux is evaluated using the **Discrete Ordinates method (Sn)** implemented in the MINARET solver. *33 energy groups are used.* The transport equation is solved for a discrete number of angular directions  $\vec{\Omega}_n$ :

$$\vec{\Omega}_n \cdot \vec{\nabla} \phi^g(\vec{r}, \vec{\Omega}_n) + \Sigma^g(\vec{r}) \phi^g(\vec{r}, \vec{\Omega}_n) = Q^g(\vec{r}, \vec{\Omega}_n)$$

**Discontinuous Galerkin Finite Element Method (DGFEM)** is applied with a triangular 2D mesh. The weak formulation of the problem is:

$$\begin{aligned} \int_{V_\alpha} d^3r [\Sigma^g(\vec{r}) \phi(\vec{r}, \vec{\Omega}_n) - \phi^g(\vec{r}, \vec{\Omega}_n) \vec{\Omega}_n \cdot \vec{\nabla}] \psi(\vec{r}) = \\ = - \int_{S_\alpha} d^2r_b \vec{\Omega}_n \cdot \vec{N}_\alpha^{out} \phi^g(\vec{r}_b, \vec{\Omega}_n) \psi(\vec{r}_b) + \int_{V_\alpha} d^3r Q^g(\vec{r}, \vec{\Omega}_n) \psi(\vec{r}) \end{aligned}$$

The flux is expanded on the polynomial basis function  $\psi(\vec{r})$ . Its degree can be zero ( $P_0$ ), one ( $P_1$ ) or two ( $P_2$ ).



In order to reduce the calculation time, *parallelization techniques* are implemented:

- ▶ angular directions are treated independently and then interfaced
- ▶ a domain decomposition method (DDM) is applied: the spatial mesh is divided into macro-domains



The normalization of the flux  $\Phi$  is of major importance in our calculations. The **constant power depletion** case is assumed. The power released will be kept the same at the beginning and at the end of the calculation stage and equal to a value  $P$ :

$$\begin{aligned} & \sum_{j=1}^J \left[ \sum_{g=1}^G \kappa_{f,j}^g \sigma_{f,j}^g(t_0) \phi^g(t_0) \right] N_j(t_0) + \sum_{j=1}^{N_{iso}} \left[ \sum_{g=1}^G \kappa_{\gamma,j}^g \sigma_{\gamma,j}^g(t_0) \phi^g(t_0) \right] N_j(t_0) = \\ & = \sum_{j=1}^J \left[ \sum_{g=1}^G \kappa_{f,j}^g \sigma_{f,j}^g(t_f) \phi^g(t_f) \right] N_j(t_f) + \sum_{j=1}^{N_{iso}} \left[ \sum_{g=1}^G \kappa_{\gamma,j}^g \sigma_{\gamma,j}^g(t_f) \phi^g(t_f) \right] N_j(t_f) = P \end{aligned}$$

where  $\kappa_{f,j}^g$  and  $\kappa_{\gamma,j}^g$  are the energy released respectively per fission and radiative capture in the energy group  $g$  of the isotope  $j$ ,  $J$  is the number of fissile isotope.

$$\begin{cases} \frac{d\vec{N}}{dt} = \bar{\bar{A}}(\lambda, \tau(t)) \cdot \vec{N}(t) \\ \vec{N}(0) = \vec{N}_0 \end{cases}$$

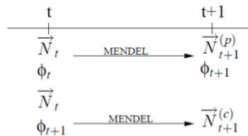
A multistep approach is used to resolve the following integral:

$$\vec{N}(t + \Delta t) = \vec{N}_0 + \int_t^{t+\Delta t} \bar{\bar{A}}(\lambda, \tau(t)) \cdot \vec{N}(t) dt$$

In order to solve numerically this integral an estimation of the time variation of the matrix  $\bar{\bar{A}}$  is required.

# MENDEL Depletion Solver

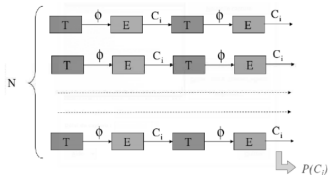
## TRIPOLI 4-D : Predictor - Corrector Method

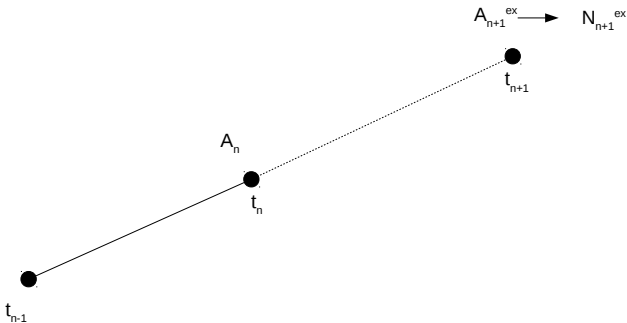


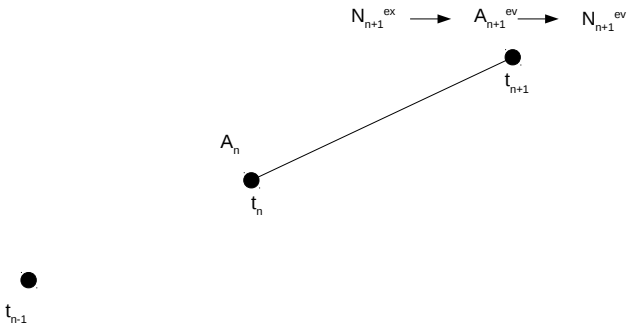
Algorithm:

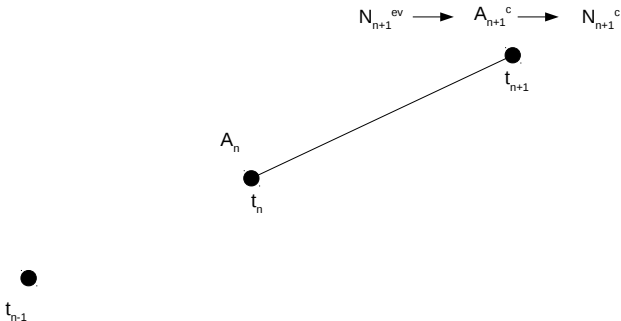
```

 $\vec{N}_0$ 
for  $n = 0$  to  $N$  do
   $\phi_n \leftarrow \text{TRIPOLI}(\vec{N}_n)$ 
   $\vec{N}_{n+1}^{(p)} \leftarrow \text{MENDEL}(\vec{N}_n, \phi_n)$ 
   $\phi_{n+1} \leftarrow \text{TRIPOLI}(\vec{N}_{n+1}^{(p)})$ 
   $\vec{N}_{n+1}^{(c)} \leftarrow \text{MENDEL}(\vec{N}_{n+1}^{(p)}, \phi_{n+1})$ 
   $\vec{N}_{n+1} = \frac{\vec{N}_{n+1}^{(p)} + \vec{N}_{n+1}^{(c)}}{2}$ 
end for
  
```

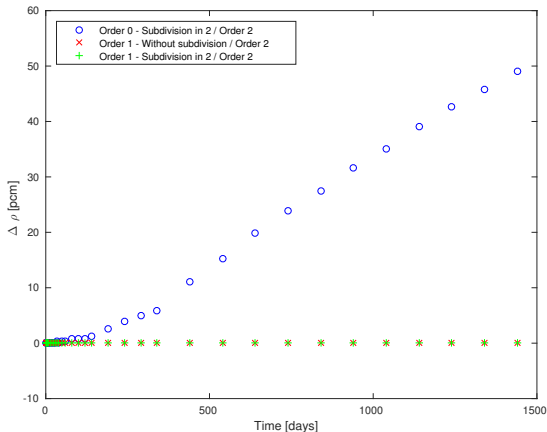












The two codes use the same numerical method to solve the integral once time dependence of matrix  $\bar{\bar{A}}$  is defined:

$$h = t_{i+1} - t_i$$

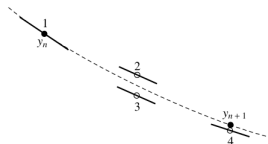
$$\vec{k}_1 = h \bar{\bar{A}}(t_i) \cdot \vec{N}_i$$

$$\vec{k}_2 = h \bar{\bar{A}}\left(t_i + \frac{h}{2}\right) \cdot \left(\vec{N}_i + \frac{\vec{k}_1}{2}\right)$$

$$\vec{k}_3 = h \bar{\bar{A}}\left(t_i + \frac{h}{2}\right) \cdot \left(\vec{N}_i + \frac{\vec{k}_2}{2}\right)$$

$$\vec{k}_4 = h \bar{\bar{A}}(t_i + h) \cdot (\vec{N}_i + \vec{k}_3)$$

$$\vec{N}_{i+1} = \vec{N}_i + \frac{\vec{k}_1}{6} + \frac{\vec{k}_2}{3} + \frac{\vec{k}_3}{3} + \frac{\vec{k}_4}{6} + O(h^5)$$



$$\begin{cases} \frac{d\vec{N}}{dt} = \bar{\bar{A}}(\lambda, \tau(0)) \cdot \vec{N}(t) \\ \vec{N}(0) = \vec{N}_0 \end{cases}$$

Matrix  $\bar{\bar{A}}$  is supposed to be constant. The exponential matrix can be introduced:

$$\vec{N}(t) = \left( e^{\bar{\bar{A}}(\lambda, \tau(0))t} \right) \cdot \vec{N}_0$$

The representation with a proper Taylor's series is:

$$e^{\bar{\bar{A}}(\lambda, \tau(0))t} = \bar{\bar{I}} + \bar{\bar{A}}t + \frac{1}{2}\bar{\bar{A}} \cdot \bar{\bar{A}}t^2 + \dots$$

“Is it possible to simplify the calculation scheme adapting it to the currently used one?”

The multiplication factor at time zero is equal to **1.40694**. This value is **17 pcm smaller** than the one presented in the previous section. *It is obtained using the same condensed cross sections for the couple of materials C1 , C1\_ABS and C2 , C2\_ABS*. These cross sections come from the condensation of an infinite fissile assembly lattice calculation.

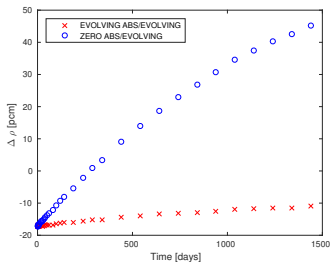
# 2D Core Plane Geometry

## New Calculation Scheme: Comparisons at 1440 days

	Peak/Lowest Value Ratio			Peak/Inner Fertile Averaged Value		
	EVOL	ZERO ABS	EVOL ABS	EVOL	ZERO ABS	EVOL ABS
U238	1.405	1.405	1.405	1.071	1.071	1.071
U235	2.191	2.192	2.190	1.734	1.735	1.731
Pu239	225	225	225	2.645	2.656	2.649
Pd105	12665	12698	12673	5.238	5.272	5.258
Tc99	2201	2206	2202	4.032	4.062	4.047
Ru101	4540	4552	4542	4.449	4.482	4.465
Rh103	8699	8721	8703	4.766	4.801	4.784

# 2D Core Plane Geometry

## New Calculation Scheme: Depletion Models



Results at 1440 days

	$k_{eff}$	$\Delta \rho [pcm]$
SIGMA EVOLVING	1.28822	/
ZERO ABS	1.28897	+45
EVOLVING ABS	1.28804	-11